J Therm Anal Calorim (2010) 101:1149–1153
DOI 10.1007/s10973-009-0659-2

Interactions between $AuCl_4^-$ and CTA^+ ions in water

Enthalpies for the formation of the precipitate

Makoto Takezaki · Hiroyuki Aoki ·
Michiko Kodama · Toshihiro Tominaga

Received: 9 October 2009 / Accepted: 14 December 2009 / Published online: 7 January 2010

Abstract The solubility of hexadecyltrimethylammonium tetrachloroaurate ($CTA{\cdot}AuCl_4$) in water was measured at different temperatures of 288.2, 293.2, 298.2, 303.2, and 308.2 K. The enthalpy change associated with the formation of the $CTA{\cdot}AuCl_4$ precipitate was estimated on the basis of the van't Hoff equation and was found to be -42.5 ± 2.8 kJ mol^{-1} at 298.2 K. The calorimetric enthalpy change for the $CTA{\cdot}AuCl_4$ precipitate formation was directly determined by isothermal titration calorimetry performed at 298.2 K and was found to agree well with that estimated from the van't Hoff equation.

Keywords Tetrachloroaurate ion · Hexadecyltrimethylammonium ion · Gold nanoparticle · Solubility · Van't Hoff enthalpy · Titration calorimetry

Introduction

Metal nanoparticles show unique properties that are different from bulk metals [1]. Recently various kinds of metal [2–7], metal oxide [8, 9], and metal sulfide [10] nanoparticles have been synthesized and characterized. Gold nanoparticles differing in both size and shape have been frequently synthesized by reducing the $AuCl_4^-$ ion in the presence of surfactants acting as protective agents or templates in the synthesis [2–7]. When alkyltrimethylammonium (RTA^+) halides are used as the protective agents, ion–pair precursors are formed, designated as $[(RTA)_m(AuCl_4)_n]^{m-n}$ ($m \geq n \geq 1$), which are then transformed into gold nanoparticles by way of a reduction process. Among the precursor species, solubility of the $RTA{\cdot}AuCl_4$ species ($m = 1$, $n = 1$) in water is low, and the solubility of the precursors increases with increasing m/n ratio. We consider that both the size and the shape of the synthesized nanoparticles are affected by both the m/n ratio and the reduction potential of the precursors $[(RTA)_m(AuCl_4)_n]^{m-n}$. From this viewpoint, a study on the interactions between the ions of RTA^+ and $AuCl_4^-$ is important to understand the mechanism of the gold nanoparticle formation.

In this study, the solubility of one of the ion–pair precursor species, hexadecyltrimethylammonium tetrachloroaurate ($CTA{\cdot}AuCl_4$), in water was determined at various temperatures using UV absorption measurements, and the van't Hoff enthalpy for the formation of $CTA{\cdot}AuCl_4$ was estimated from the temperature dependence of the solubility. In addition, the enthalpy change associated with the $CTA{\cdot}AuCl_4$ precipitate formation was directly determined with isothermal titration calorimetry (ITC).

Experimental

Sodium tetrachloroaurate dihydrate ($NaAuCl_4{\cdot}2H_2O$, Nacalai Tesque, guaranteed reagent) was used without further purification. Hexadecyltrimethyl-ammonium chloride (CTAC,

M. Takezaki · T. Tominaga (✉)
Department of Applied Chemistry, Okayama University of Science, 1-1 Ridai-cho, Kita-ku, Okayama 700-0005, Japan
e-mail: tominaga@dac.ous.ac.jp

H. Aoki · M. Kodama
Department of Biochemistry, Okayama University of Science, 1-1 Ridai-cho, Kita-ku, Okayama 700-0005, Japan

Tokyo Kasei, extra pure reagent) was recrystallized four times with a methanol/acetone mixture. Water used in this study was obtained by distilling de-ionized water twice.

The exact number of water molecules in the purchased $NaAuCl_4{\cdot}2H_2O$ was determined to be 2.4-mol H_2O per mole of $NaAuCl_4$ using a themogravimetry apparatus (Rigaku, TG8120). On this basis, the molar extinction coefficient of the $AuCl_4^-$ anion was determined at the UV absorption band maximum at 213 nm. The UV absorption measurements were performed with Hitachi spectrophotometer (U-3310). When the absorbance was plotted against the $NaAuCl_4$ concentration, a good straight line was obtained up to the concentration of 5.0×10^{-5} M (1 M = 1 mol L^{-1}), and the molar extinction coefficient of $AuCl_4^-$ was estimated to be $1.65 \pm 0.05 \times 10^4$ M^{-1} cm^{-1}.

In order to prepare the precursor $CTA{\cdot}AuCl_4$ ($m = 1$, $n = 1$) precipitate, CTAC aqueous solution and $NaAuCl_4$ aqueous solution were mixed at an equimolar amount. The precipitate recovered by filtration was then washed with water three times. The solubility of the $CTA{\cdot}AuCl_4$ precipitate in water at different temperatures was determined with the molar extinction coefficient of $AuCl_4^-$ at a wavelength of 213 nm. In this experiment, the $CTA{\cdot}AuCl_4$ precipitate was stirred for at least 3 days in a water thermostat maintained at desired temperatures of 288.2, 293.2, 298.2, 303.2, and 308.2 K, respectively, and was then stored for 3 days in the water thermostat kept at the respective temperatures. Undissolved precipitate was removed by filtration using a cellulose acetate membrane of 0.45 μm pores (Advantec, DISMIC-45cs), after which UV absorption measurements were made.

ITC was performed using a high-precision VP-ITC titration calorimeter of a heat compensation type (Microcal Inc., Northampton, MA) at 298.2 K. The instrument was electrically calibrated, at the sensitivity range under investigation, internally using the VP-ITC's integral electric heater, as recommended by the manufacturers. In this calorimetric experiment, 10 μL (0.1 μmol CTAC) of 10-mM CTAC aqueous solution in the injection syringe was injected stepwise into the calorimetric cell containing 0.5-mM $NaAuCl_4$ solution (cell volume 1.429 mL). Prior to this titration, to obtain the heat of dilution for 0.5-mM $NaAuCl_4$ aqueous solution, we performed stepwise injections of a desired amount of water into the cell containing the $NaAuCl_4$ solution. In addition, both the heat of disruption of the CTAC micelles and the critical micelle concentration (CMC) of the surfactant were investigated by injecting stepwise a desired amount of 10-mM CTAC solution in the syringe into the cell containing distilled water. The data were processed using Origin software provided with the equipment.

Results and discussion

Solubility and the van't Hoff enthalpy for the formation of the $CTA{\cdot}AuCl_4$ precipitate

The precipitate formation/dissolution equilibrium is expressed as

$$\mathrm{CTA} \cdot \mathrm{AuCl}_{4\mathrm{solid}} \underset{K}{\overset{S}{\longleftrightarrow}} \mathrm{CTA}^+_{\mathrm{aq}} + \mathrm{AuCl}^-_{4\mathrm{aq}} \tag{1}$$

where the solid state $CTA{\cdot}AuCl_{4solid}$ is in equilibrium with $CTA{\cdot}AuCl_4$ in a saturated aqueous solution and is assumed to completely dissociate into CTA^+ and $AuCl_4^-$ ions in the saturated solution, S is the solubility product, and K is the precipitate formation constant that is the reciprocal of S. Molar concentrations of $AuCl_4^-$ in saturated solutions were determined at 288.2, 293.2, 298.2, 303.2, and 308.2 K with the molar extinction coefficient of $AuCl_4^-$. The resultant solubility values are given in Table 1 together with the K values. The ln K values are plotted in Fig. 1 against the reciprocal temperature, where fairly good linearity is observed. From the fitted straight line, we estimated the van't Hoff enthalpy, ΔH^0, for the formation of the $CTA{\cdot}AuCl_4$ precipitate according to Eq. 2

$$\left[\frac{\partial \ln K}{\partial(1/T)}\right]_{\mathrm{P}} = -\frac{\Delta H^0}{R} \tag{2}$$

where R is the gas constant, and T is the absolute temperature. The resultant value of ΔH^0 is found to be -42.5 ± 2.8 kJ mol^{-1}.

Careful examination of Fig. 1, however, shows that the experimental points are concave downward. Using the empirical equation [11, 12]

$$\Delta G^0 = -RT \ln K = A_0 + A_1 T + A_2 T^2 \tag{3}$$

we obtained the values 1.140×10^5, 1.081×10^3 kJ mol^{-1} K^{-1}, and 1.763 kJ mol^{-1} K^{-2} for A_0, A_1, and A_2, respectively. ΔH^0 values were calculated using the relation

$$\Delta H^0 = A_0 - A_1 T^2 \tag{4}$$

The ΔH^0 values obtained at respective temperatures are listed in Table 2. The absolute values of the exothermic

Table 1 Solubility of $CTA{\cdot}AuCl_4$ in water and the precipitate formation constant K

T/K	$[CTA{\cdot}AuCl_4]$/M[a]	K/M^2
288.2	2.26×10^{-5}	1.96×10^9
293.2	2.66×10^{-5}	1.41×10^9
298.2	2.92×10^{-5}	1.17×10^9
303.2	3.42×10^{-5}	0.85×10^9
308.2	4.04×10^{-5}	0.61×10^9

[a] 1 M = 1 mol L^{-1}

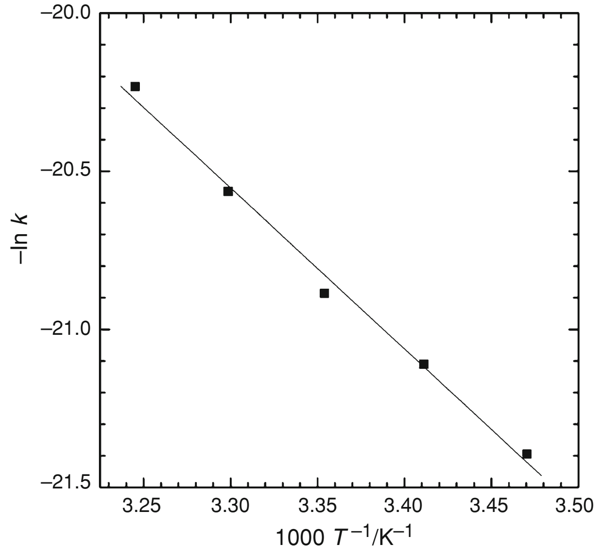

Fig. 1 Formation constant of the $CTA{\cdot}AuCl_4$ precipitate in water as a function of temperature

Table 2 Temperature dependence of ΔH^0

T/K	ΔH^0/kJ mol^{-1}
288.2	−32.5
293.2	−37.6
298.2	−42.8
303.2	−48.1
308.2	−53.5

enthalpy are seen to decrease with decreasing temperature. This must reflect the hydrophobic hydration of the alkyl chain of the CTA^+ ion in water. The same tendency is well known for the solubility of long-chain alkanols and alkylbenzenes (water–organic liquid equilibrium) [13] and the temperature dependence of the CMC (water–micelle equilibrium) [14–18].

ITC and calorimetric enthalpy change for the formation of the $CTA{\cdot}AuCl_4$ precipitate

The present microcalorimetric titration experiments were performed only for a temperature at 298.2 K. Figure 2a shows the heat flow curves obtained upon stepwise injections of 5 μL of 10-mM CTAC solution into the cell containing only water, thus, in the absence of $NaAuCl_4$. As shown in Fig. 2a, a large endothermic peak, which is due to a rupture of the micelles into monomers, was observed up to injections of the first 20 aliquots. After this, the peak gradually becomes smaller in area. In Fig. 2b, the cumulative enthalpy change (ΔH) obtained from Fig. 2a is plotted against the CTAC concentration (C) and is shown to increase linearly up to around 0.74 mM, after which the ΔH curve increases gently and then reaches a plateau (thus, becomes parallel to the abscissa). The slope of the straight line of ΔH versus C curve gives the molar enthalpy change associated with the de-micellization of CTAC. The resultant value of ΔH is 1.71 kJ mol^{-1}, which is somewhat smaller than values of 2.3 kJ mol^{-1} [19] and 4.4 kJ mol^{-1} [20] reported by other workers. On the other hand, the CMC of CTAC was determined graphically by extrapolating the two straight lines, one from 0 to 0.74 mM and the other from 1.14 to 1.82 mM [21, 22]. Thus, the concentration of the intersection point for the extrapolated lines (dashed lines) gives a CMC of CTAC. The resultant CMC of CTAC was 0.83 mM, which is a little smaller than the generally accepted value of 1.2 mM [20, 23, 24].

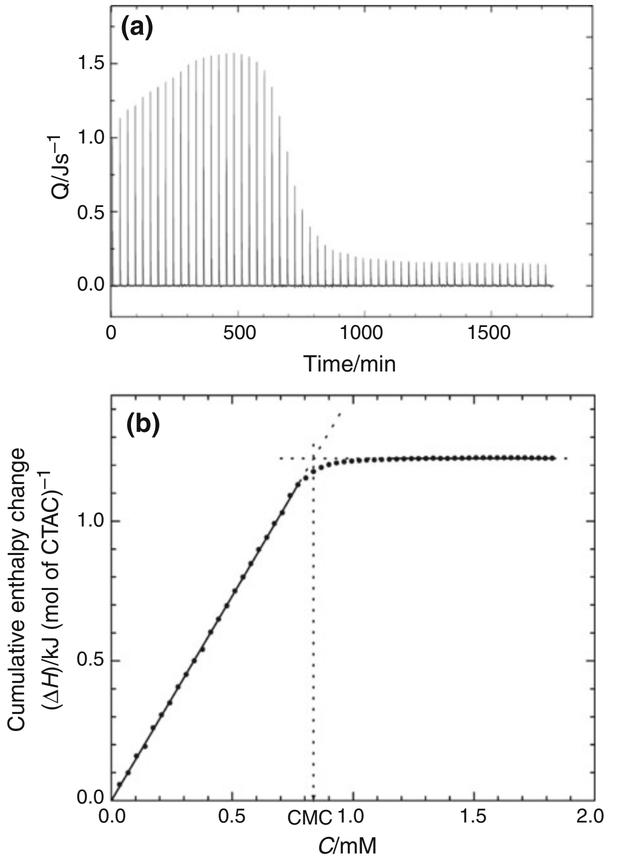

Fig. 2 ITC experiment for de-micellization of CTAC at 298.2 K. Heat flow peaks obtained upon injection of a series of 5-μL aliquots of 10-mM CTAC solution into 1.442-mL water in the calorimeter cell (**a**). The cumulative enthalpy change for demicellization of CTAC as a function of the CTAC concentration in the calorimeter cell (**b**)

Figure 3a shows the calorimetric titration profile due to injections of 10-mM CTAC solution into the cell containing 0.5-mM $NaAuCl_4$ solution. In Fig. 3b, the exothermic heats per mole of CTAC obtained for each injection are plotted as a function of molar ratio of CTA^+ to $AuCl_4^-$ in the calorimeter cell. In order to obtain both the enthalpy

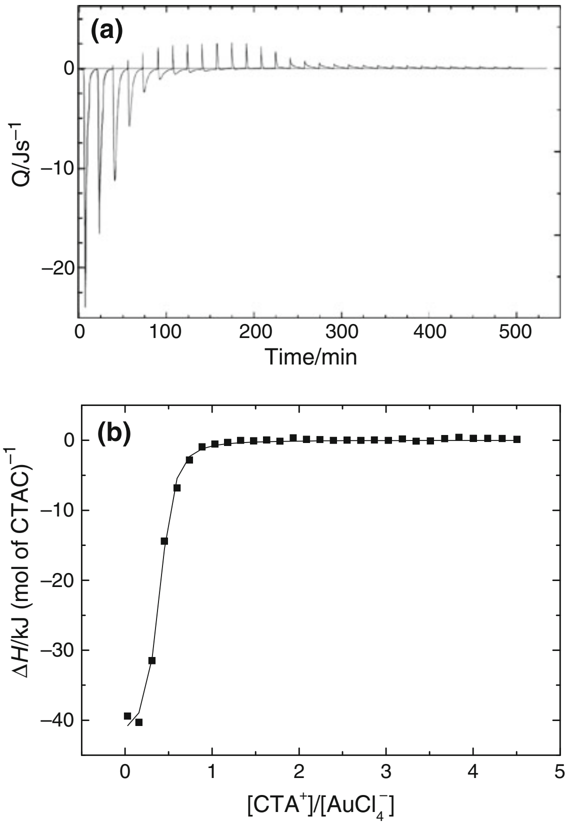

Fig. 3 ITC experiment for the formation of CTA·AuCl$_4$ precipitate at 298.2 K. Heat flow peaks obtained upon injection of a series of 10-μL aliquots of 10-mM CTAC solution into 1.442 mL of 0.5-mM AuCl$_4^-$ in the calorimeter cell (**a**). The heats of injection per mole of injected CTAC as a function of molar ratio of CTA$^+$ to AuCl$_4^-$ in the calorimeter cell (**b**)

change (ΔH^0) and the equilibrium constant (K') for the CTA·AuCl$_4$ precipitate formation, the theoretical curve best fitted to experimental data was determined using a computer program (Origin) supplied with the Microcal calorimeter, and the resultant theoretical curve gave ΔH^0 (i.e., calorimetric enthalpy) of −43.3 kJ per mole of CTA·AuCl$_4$ and K' value of 9.5×10^4 $M^{-1\cdot}$ A point to be noted is that the calorimetric enthalpy (−43.3 kJ mol^{-1}) is very close to the van't Hoff enthalpy (−42.5 kJ mol^{-1}) obtained from the solubility measurements. It has been reported that the van't Hoff enthalpy and calorimetric enthalpy do not agree with each other [25]. In the present system, however, the one phase is a solid phase having unit activity and the other phase of saturated solution is a very dilute aqueous solution where the activity coefficients of both CTA$^+$ and AuCl$_4^-$ ions are close to one. This fact would be related to the agreement of the van't Hoff enthalpy and the calorimetric enthalpy obtained in this study.

We are in the process to determine the equilibrium constants between species, $[(\mathrm{CTA})_m(\mathrm{AuCl}_4)]^{m-1}$, where the m value is changed from 1 to 2, 3, and larger. This study is a first step to obtain information to clarify the mechanism of the nanoparticle formation.

Conclusions

The solubility of CTA·AuCl$_4$ was measured over the temperatures ranging from 288.2 to 308.2 K, and the enthalpy change (van't Hoff enthalpy) for the formation of the CTA·AuCl$_4$ precipitate was obtained. The enthalpy change for the formation of the CTA·AuCl$_4$ precipitate was also obtained directly by ITC measurements at 298.2 K and showed a good agreement with the van't Hoff enthalpy at the same temperature. The results obtained in this study are expected to provide useful information in understanding the mechanism of gold nanoparticle formation.

Acknowledgements We thank Prof. M. Fukuhara, Okayama University of Science, for thermal gravimetric measurements. This study was supported by "High-Tech Research Center" Project for Private Universities: matching fund subsidy from MEXT (Ministry of Education, Culture, Sports, Science and Technology), 2006-2008.

References

1. Schmid G, editor. Nanoparticles: from theory to application. Weinheim: Wiley-VCH; 2004.
2. Jana NR, Gearheart L, Murphy CJ. Seeding growth for size control of 5–40 nm diameter gold nanoparticles. Langmuir. 2001;17:6782–6.
3. Torigoe K, Esumi K. Preparation of colloidal gold by photoreduction of tetracyanoaurate(−)-cationic surfactant complexes. Langmuir. 1992;8:59–63.
4. Yu YY, Chang SS, Lee CL, Wang CR. Gold nanorods: electrochemical synthesis and optical properties. J Phys Chem B. 1997;101:6661–4.
5. Wang ZL, Gao RP, Nikoobakht B, El-Sayed MA. Surface reconstruction of the unstable 110 surface in gold nanorods. J Phys Chem B. 2000;104:5417–20.
6. Kim F, Song JH, Yang P. Photochemical synthesis of gold nanorods. J Am Chem Soc. 2002;124:14316–7.
7. Takezaki M, Kida R, Kato Y, Tominaga T. Preparation of triangular gold nanoparticles by chemical and photoreduction methods. Chem Lett. 2009;38:1022–3.
8. Kubota M, Kanazawa Y, Nasu K, Moritake S, Kawaji H, Atake T, et al. Effect of heat treatment on magnetic $MgFe_2O_4$ nanoparticles. J Therm Anal Calorim. 2008;92:461–3.
9. More A, Verenkar VMS, Mojumdar SC. Nickel ferrite nanoparticles synthesis from novel fumarato-hydrazine precursor. J Therm Anal Calorim. 2008;94:63–7.
10. Fini P, Depalo N, Comparelli R, Curri ML, Striccoli M, Castagnolo M, et al. Interactions between surfactant capped CdS nanoparticles and organic solvent. J Therm Anal Calorim. 2008;92:270–7.
11. Wilhelm E, Battino R. Thermodynamic functions of the solubilities of gases in liquids at 25 °C. Chem Rev. 1973;73:1–9.
12. Osborne JC, Palumbo G, Brewer HB, Edelhoch H. The thermodynamics of the self-association of the reduced and

carboxymethylated form of ApoA-II from the human high density lipoprotein complex. Biochemistry. 1976;15:317–20.

13. Shinoda K. “Iceberg” formation and solubility. J Phys Chem. 1977;81:1300–2.
14. Flockhart BD. The effect of temperature on the critical micelle concentration of some paraffin-chain salts. J Colloid Interface Sci. 1961;16:484–92.
15. Robins DC, Thomas IL. The effect of counterions on micellar properties of 2-dodecylaminoethanol salts I. Surface tension and electrical conductance studies. J Colloid Interface Sci. 1968; 26:407–14.
16. Barry BW, Russell GFJ. Prediction of micellar molecular weights and thermodynamics of micellization of mixtures of alkyltrimethylammonium salts. J Colloid Interface Sci. 1972;40:174–94.
17. Evans DF, Wightman PJ. Micelle formation above 100°C. J Colloid Interface Sci. 1982;86:515–24.
18. Shinoda K, Kobayashi M, Yamaguchi N. Effect of “iceberg” formation of water on the enthalpy and entropy of solution of paraffin chain compounds: the effect of temperature on the critical micelle concentration of lithium perfluorooctane sulfonate. J Phys Chem. 1987;91:5292–4.
19. Paredes S, Tribout M, Sepulveda L. Enthalpies of micellization of the quaternary tetradecyl- and cetyltrimethylammonium salts. J Phys Chem. 1984;88:1871–5.
20. Jiang N, Li P, Wang Y, Wang J, Yan H, Thomas RK. Aggregation behavior of hexadecyltrimethylammonium surfactants with various counterions in aqueous solution. J Colloid Interface Sci. 2005;286:755–60.
21. van Os NM, Daane GJ, Haandrikman G. The effect of chemical structure upon the thermodynamics of micellization of model alkylarenesulfonates: III. Determination of the critical micelle concentration and the enthalpy of demicellization by means of microcalorimetry and a comparison with the phase separation model. J Colloid Interface Sci. 1991;141:199–217.
22. Blandamar MJ, Briggs B, Cullis PM, Engberts BFN. Titration microcalorimetry of mixed alkyltrimethylammonium bromide surfactant aqueous solutions. Phys Chem Chem Phys. 2000; 2:5146–53.
23. Mukerjee P, Mysels KJ. Critical micelle concentration of aqueous surfactant systems. In: National Standard Reference Data Series, vol. 36. Washington, DC: National Bureau of Standards; 1971.
24. Malliaris A, Le Moigne J, Sturm J, Zana R. Temperature dependence of the micelle aggregation number and rate of intramicellar excimer formation in aqueous surfactant solutions. J Phys Chem. 1985;89:2709–13.
25. Mizoue LS, Tellinghuisen J. Calorimetric vs. van’t Hoff binding enthalpies from isothermal titration calorimetry: Ba^{2+}-crown ether complex. Biophys Chem. 2004;100:15–24.